International Journal of Pharmaceutics 550 (2018) 207–215

Contents lists available at ScienceDirect

International Journal of Pharmaceutics

journal homepage: www.elsevier.com/locate/ijpharm

Diffusion through the *ex vivo* vitreal body – Bovine, porcine, and ovine models are poor surrogates for the human vitreous

Sara Shafaie[a], Victoria Hutter[a], Marc B. Brown[a,b], Michael T. Cook[a], David Y.S. Chau[a,*]

[a] Research Centre in Topical Drug Delivery and Toxicology, Department of Pharmacy, Pharmacology and Postgraduate Medicine, School of Life and Medical Sciences, University of Hertfordshire, College Lane, Hatfield AL10 9AB, UK

[b] MedPharm Ltd Unit 3 Chancellor Court, 50 Occam Road, Surrey, Guildford GU2 7YN, UK

ARTICLE INFO

Keywords:
Franz cell
Hyaluronic acid
Hydrogel
Ocular drug delivery
Permeability
Diffusion
Rheology
Vitreous substitute

ABSTRACT

The human vitreous humour is a complex gel structure whose composition and physical properties can vary considerably from person to person and also change with age. To date, the viscoelastic properties of the human vitreous gel has not been thoroughly investigated and despite many years of intensive research, an ideal vitreous substitute remains a challenge. Understanding the physical structure and properties of the vitreous is of fundamental and therapeutic interest, providing a clear insight into diffusion and transport of administered ophthalmic drug molecules into the vitreous. A number of mammalian surrogates, mainly bovine, porcine and ovine vitreous humours have been used in the literature as a means of studying ophthalmic drug transport and diffusion. In this study, the mechanical, physical and rheological properties of ovine, porcine, and bovine surrogates were investigated and compared to human vitreous. In addition, a bespoke Franz cell construct was used to compare the diffusion of a model drug (fluorescein) through vitreous samples. Despite the similarity in rheological properties between bovine, porcine and human vitreous samples, diffusion of fluorescein through the different vitreous samples revealed great differences in values of steady-state flux and diffusion coefficient. In addition, a first-generation vitreous mimic, composed of 4.5 mg/mL hyaluronic acid with complex viscosity of 0.3 ± 0.01 Pa has been evaluated and was demonstrated to be a better mimic of the human vitreous than the mammalian samples investigated.

1. Introduction

Ocular diseases affect the quality of life of millions of people worldwide. These diseases can affect both the anterior and posterior segments of the eye, such as cataracts and age-related macular degeneration, respectively. There are many challenges associated with topical drug formulations for treatment of posterior-related ocular diseases, including poor drug penetration and short residence time. Drug treatment via the systemic route of administration has its own drawbacks; including blood-retinal barriers, and unwanted side effects as a result of the large doses required (Duvvuri et al., 2003).

An alternative route for drug delivery to the posterior segment of the eye is by intravitreal injections and implants, which introduce drug directly into the vitreous body with lower risk of systemic side effects (Käsdorf et al., 2015). As such, the vitreous body has become an attractive location for the administration of injections or implants in modern ophthalmology. Such intravitreal dosage forms are loaded with active agents which may disperse as a single bolus (e.g. gentamicin), or are released over a prolonged period of time (e.g. Iluvien® implant). In order to predict the transport of drug within the vitreous, it is essential to understand the nature and interactions among various processes that can occur within the vitreous. Consequently, a test model that simulates the *in vivo* situation is needed to assess the diffusion behaviour of drugs and dosage forms within the vitreous chamber.

The human vitreous chamber is a sphere about 16.5 mm in axial diameter that occupies a volume of about 4.5 mL (Sharif-Kashani et al., 2011). The vitreous hydrogel component, with a water content of > 98%, occupies a significant volume in the eye which fills the space between the lens and retina and acts as a filling substance to maintain structural integrity and intraocular pressure (Donati et al., 2014; Shafaie et al., 2016). Its gel structure is mainly composed of different types of collagen (Type II, IX, V/IX, and IV), with a total concentration of approximately 300 μg/mL (Le Goff and Bishop, 2008). Although fibrillary collagens, such as type II collagen, have a tendency to fuse on contact, vitreal type IX collagen acts as a shield on the surface of the vitreous collagen fibrils and prevents fusion between fibrils. With aging,

* Corresponding author.
E-mail address: d.chau@herts.ac.uk (D.Y.S. Chau).

https://doi.org/10.1016/j.ijpharm.2018.07.070
Received 16 April 2018; Received in revised form 24 July 2018; Accepted 25 July 2018
Available online 21 August 2018

however, such shielding property is lost and type II collagen becomes predisposed to fuse with adjacent fibrils on contact (Bishop et al., 2004). In addition to collagen, glycosaminoglycans (GAGs) such as hyaluronic acid (HA), heparin sulfate (HS), and chondroitin sulfate are also present (Käsdorf et al., 2015). Therefore, the vitreous can be known as a hydrogel comprised of water in a collagen-glycosaminoglycan network (CGN). Within such network, collagen fibrils are packed parallel and are separated by random coil of HA. The density of CGN is not uniform across they eye with a predominant orientation of fibrils and fibres anterior-posterior (Kodama et al., 2013). Additionally, the concentration of HA varies from 65 to 400 μg/mL in adult human, 50–570 μg/mL in bovine vitreous and 160 μg/mL in porcine vitreous Reardon et al. (1998). This large variation could be related to the heterogeneous distribution of vitreous components throughout the bulk hydrogel (Balazs et al., 1959), as well as age-related changes in its composition (Denlinger et al., 1980). Furthermore, it has been reported that the micro-rheology of the bovine vitreous humour undergoes a length scale dependent transition; changing from a viscous liquid state to an elastic solid profile (Xu et al., 2013). Overall, this gelatinous structure does not have a homogenous density and appears denser adjacent to the vitreous cortex and more at the ora serrata (Green and Sebag, 2006). The network of collagen fibrils has been recognised to serve the load-bearing function because the vitreous does not collapse during enzymatic removal of hyaluronan but dissolves completely after digestion with collagenase, converting the vitreous into a viscous liquid (Bishop, 2000; Pirie et al., 1948).

Previously, it has been shown that in human vitreous, collagen fibrils are presented in loose and roughly parallel bundles with a considerable gap from their adjacent bundles and with some at right angles to the others (Fig. 1). Such pattern of parallel collagen fibrils tied together by proteoglycan bridges is similar to the pattern seen in cornea where parallel collagen fibrils are also bridged by proteoglycans (Scott, 1992). In addition, it was suggested that swollen and charged polysaccharide chains of hyaluronan simply hydrate the vitreous network and help to prevent aggregation by filling the space between the fibrils (Nickerson et al., 2008). Another important characteristic of the CGN is its porous structure which changes throughout the eye with a change in the CGN density. For instance, in the central vitreous with a low CGN density, pore size can vary from 500 nm to over 1 μm (Xu et al., 2013). Such properties of the vitreous are essential to provide structural support for the growth of the eye, to maintain a clear path to the retina, and to support the various ocular tissues during physical activity (Sebag and Balazs, 1989).

To date, a significant amount of work has been dedicated to the study of the anatomical and physiological structure of the vitreous. Amongst which, there have been few studies that have investigated diffusion through the vitreous humours, typically using *ex vivo* animal vitreous. For instance, Käsdorf et al. (2015) have studied FITC-dextran and peptide penetration into the ovine vitreous humour. Ohtori and Tojo measured the diffusion coefficient of dexamethasone sodium *m*-sulfobenzoate in rabbit vitreous by designing a glass ring diffusion apparatus (Ohtori and Tojo, 1994). A study by Gisladottir et al. (2009) used a diffusion cell with a middle chamber to study diffusion of dexamethasone through saline solution with different concentrations of hyaluronan as well as porcine vitreous humour. Most previous work on diffusion through vitreous have used fluorescein as a model compound (Xu et al., 2000). For instance, as injections of fluorescein sodium solution into either a PAA-gel or porcine vitreous humour has been used to measure diffusion through vitreous (Loch et al., 2012). In addition, in a study by Tan *et al.* (2011) sodium fluorescein was used as a model compound to assess the impact of partial vitreous liquefaction on the intravitreal movements of molecules with different molecular weights. In another study by Xu et al. (2013), diffusion of polystyrene nanoparticles of various sizes and surface chemistries through the fresh ex vivo bovine vitreous have been studied (Xu et al., 2013). Most recently, liposome diffusion coefficients in the intact vitreous of the *ex vivo* porcine eyes have been previously studied via fluorescence correlation spectroscopy. In this study, a modified Miyake-apple technique was used to introduce a window into the vitreous to minimise the disruption of the fine structure of the vitreous (Eriksen et al., 2017). Due to the molecular size of sodium fluorescein, it can be used as a representative compound to many steroids and intravitreal antimicrobial agents used in the treatments of ocular infection and inflammation (Tan et al., 2011).

To our knowledge, due to the limited availability of fresh human vitreous humour, there has not yet been any published studies on diffusion through human vitreous humour. In the presented study, the diffusion of fluorescein through human, bovine, porcine, and ovine vitreous has been studied, as well as the rheological properties of these gels. Although the macromolecular components of the vitreous gel are similar in all species, the concentration of the main components such as HA and collagen varies in different species and regionally within each sample (Table 1), which may lead to differences in rheology and diffusion. In addition, a vitreous mimic composed of hyaluronic acid has been developed and evaluated. This raises the possibility of the development of more suitable candidates that represent the physio-chemical and rheological characteristics of the human vitreous humour which could thereafter be incorporated within an *in vitro* ocular model for drug delivery and permeability studies of novel ophthalmic formulations.

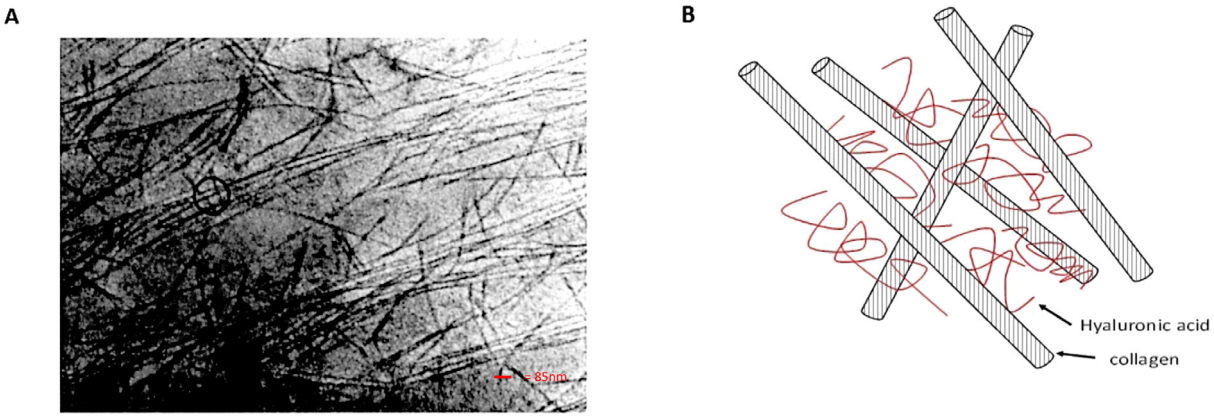

Fig 1. A) An electron micrograph of human vitreous, X 68,000. Collagen fibrils demonstrate a roughly parallel orientation in groups of two or three or more with some groups in an orthogonal orientation to other groups shown as ringed (Scott, 1992). Scale bar represents 85 nm. B) A schematic presentation of the network structure of the vitreous. The vitreous is composed of a network of collagen fibrils interspersed with hyaluronic acid (Nickerson et al., 2008).

Table 1
Collagen and HA compositions in human, porcine, bovine, and ovine vitreous humours (Käsdorf et al., 2015; Vedadghavami, 2015; Noulas et al., 2004; Kogan et al., 2007).

Vitreous	HA (μg/mL)	Collagen (μg/mL)
Human	140–340	280–1360
Porcine	160	150
Bovine	50–570	684
Ovine	100–1070	384

2. Materials and methods

Phosphate buffered saline (PBS, pH 7.4) and fluorescein sodium salt were purchased from Sigma Aldrich (Poole, Dorset, UK). Sodium hyaluronate 95% (Mw: 53.2 kDa, PDI: 3.70, determined by gel-permeation chromatography relative to poly(ethylene glycol) standards) was purchased from Fisher Scientific (Leicestershire, UK). Bovine, porcine and ovine eyes were sourced from Wetlab Ltd (Warwick, UK). Human eye globes were obtained through Moorfields Biobank (London, UK) (REC reference: 15/SW/0104, IRAS Project ID: 49666, BBR: 10/H0106/57-2016ETR63). In total, vitreous humour from both eyes of three male donors aged 48, 61, and 70 and two female donors aged 71 and 92 were used in this work. Franz cell studies used Visking Dialysis Tubing (molecular weight cut off 12,000–14,000 Daltons) which was purchased from Medicell membrane Ltd (London, UK). A modified Franz cell set up was purchased from Soham Scientific (UK), made to the authors' specification. Unless otherwise stated, all lab consumables and reagents were purchased from Sigma Aldrich (Poole, Dorset, UK) and used as supplied.

2.1. Vitreous humour extraction

In order to extract vitreous humour, a small incision was made on the lateral side of the eye using a scalpel. Vitreous humour was gently extracted on to a petri dish (Fig. 2), and non-vitreous parts attached to it, including iris and lens were further detached. Care was taken during extraction as to perform this procedure to minimise any structural damage. Extracted vitreous was stored in the fridge at 2–8 °C in sterile containers. Tests were performed within 12 h post extraction.

2.2. Rheology of vitreous

The viscosities of extracted vitreous humours were first analysed by performing an oscillatory stress sweep. An AR-G2 AR 1500ex rheometer (TA instruments) was used with a 40 mm parallel plate and a geometry gap of 600 mm, equilibrated at 34 °C for 2 min, followed by oscillation from 0.01 to 100 Pa at 1 Hz. Following the stress sweep, freshly-excised samples were subjected to a frequency sweep at a stress from the linear viscoelastic region (LVR) of the stress sweep, between 0.1 and 10 Hz. In order to prevent water evaporation and liquid loss of the vitreous during the experiment, a solvent trap seal was used to enclose the test chamber. Raw data were analysed using TA Advantage software v5.5.22. Samples were analysed in triplicate and the average of three readings were recorded.

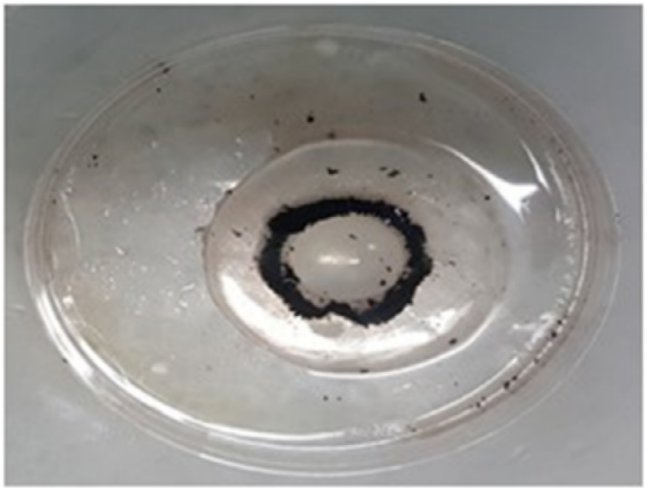

Fig 2. Extracted bovine vitreous humour from a frozen sample, attached to the lens and iris.

2.3. Hyaluronic acid vitreous mimic preparation

Different concentrations of HA in PBS ranging from 1 mg/mL to 10 mg/mL was prepared. Briefly, sodium hyaluronate was weighed and mixed with cold PBS. The sample was then stirred at 1000 RPM for 20 min until all the sodium hyaluronate powder was completely dissolved in PBS. The sodium hyaluronate solutions were then studied by rheometry to identify the concentration necessary to match the viscosity of the solutions to the human vitreous (at 1 Hz).

2.4. Texture analyser

A compression test on vitreous humour substitutes was performed using a texture analyser to measure the mechanical properties of vitreous humours. In a 6-well cell culture plate, 4 mL of sample was placed, and controlled forces were applied to the sample using a polypropylene probe with 17 mm internal diameter. The samples' response in the form of force, deformation and time was recorded. The hardness of each sample was determined as the peak force during the first compression. Results were recorded and evaluated by the Texture Expert 1.22 software.

2.5. Diffusion studies

In vitro diffusion studies were performed using a bespoke Franz cell construct compromising three main compartments; a donor chamber, a middle chamber containing vitreous, and a receiver chamber (Fig. 3). The middle chamber containing vitreous humour had a cross-sectional area of 1 cm^2 and a height of 1.5 cm. After filling the middle chamber with vitreous, a cellulose dialysis membrane was placed on both top and bottom parts of the chamber and was sealed against the donor and receiver chambers using parafilm. The receiver chamber contained PBS maintained at 34 °C ± 0.5 °C as per natural temperature of the eye (Landers et al., 2012; Rosa et al., 2015). The membrane was equilibrated at 34 °C before the donor chamber was filled with an "infinite dose" of 2 mL fluorescein solution in PBS (2 mg/mL). To ensure that diffusion through the vitreous was rate-limiting, the middle chamber was filled with PBS as a control. Over time, the fluorescent dye diffused through the membrane and vitreous and subsequently entered the receiver chamber. Samples, 3 mL each time, were taken periodically from the sample port in the receiver chamber while same volume of fresh and pre-warmed PBS was added to maintain sink conditions. The amount of fluorescent dye permeated through was quantified spectrophotometrically at 489 nm using a T80 UV–VIS spectrometer (PG Instruments Ltd., Leicestershire, England).

2.6. Calculations of steady-state flux and diffusion coefficient

Fick's first law states that the flux, J, is proportional to the concentration gradient (dC/dx) of the compound within a given medium as defined in Eq. (1):

$$J = -D\left(\frac{dC}{dx}\right) \quad (1)$$

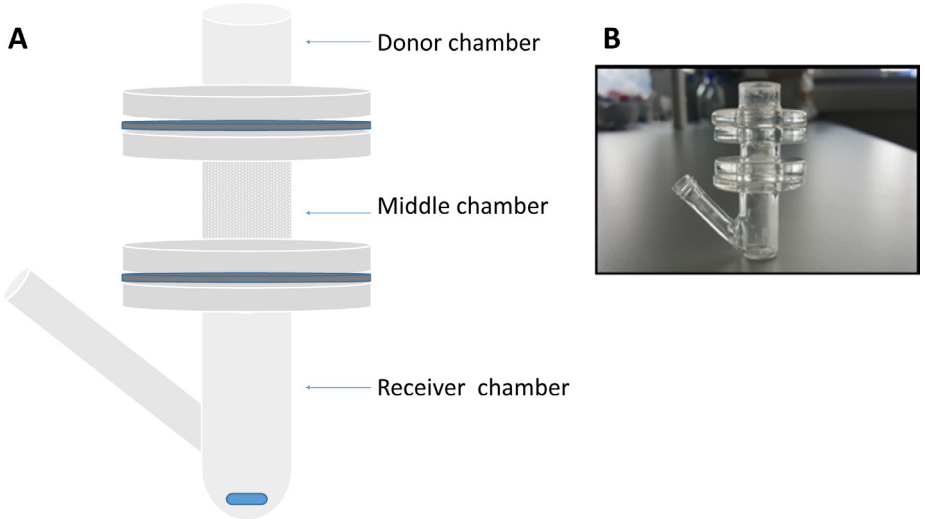

Fig 3. A) A schematic presentation of the novel in-house Franz-cell construct with a middle chamber filled with either PBS or vitreous humour. The donor chamber has a 2 mg/mL solution of fluorescein in PBS (2 mL). The receiver chamber contained PBS (3 mL) and two visking dialysis membranes encapsulate the middle chamber (MWCO 12,000–14,000 Daltons). B) Photograph of assembled Franz-cell construct.

J can be calculated by the amount of fluorescein passing through the unit cross section (S) of membrane barrier in unit time (t) as defined in Eq. (2):

$$J = \left[\frac{dM}{dt}\right]\frac{1}{S} \tag{2}$$

Steady-state flux (J) through the middle chamber filled with different mammalian vitreous was calculated by plotting the cumulative quantity of fluorescein (μg) present in receiver chamber vs time (h) divided by the middle chamber's cross section (1 cm^2). Consequently, diffusion coefficients of fluorescein in each sample were calculated using the lag time equation defined in Eq. (3) where L is lag time, D is diffusion coefficient, and h is the height of middle chamber.

$$D = \frac{h^2}{6L} \tag{3}$$

2.7. Cryo-scanning electron microscopy

Vitreous humour samples were held inside two metal rivets and flash frozen in liquid nitrogen. Samples were then transferred to the GATAN ALTO 2500 cryo prep chamber and fractured between the two rivets using a scalpel. Water was removed by etching for 45 min at −95 °C then samples were sputter coated with a thin layer of Au-Pd. The samples were imaged using a JEOL JSM 6700F scanning electron microscope at 5 kV.

2.8. Statistical analysis

Samples were analysed in at least triplicate and the results are presented as mean ± standard deviation. Any statistical significance were analysed using one-way ANOVA with Bonferroni post-hoc test. Statistical significance is indicated with (*) for $p < 0.05$, (**) for $p < 0.01$, and (***) for $p < 0.001$.

3. Results

3.1. Rheological properties: oscillatory stress sweep (OSS)

Rheological properties of human, bovine, porcine and ovine vitreous humours (VH) and HA were characterised using oscillatory stress sweep test (Fig. 4). Applied oscillatory stress, ranged from 0.01 to 100 Pa, is low at the early stages of the test to preserve structure but as the test progresses the increase in applied stress causes disruption of intermolecular structure manifested as a decrease in elasticity. Storage (G′) and loss (G″) moduli and the magnitude of the complex viscosity [η*] were obtained as a function of oscillatory stress at a constant frequency of 1 Hz.

Complex viscosity of HA in PBS at different concentrations ranging from 1 mg/mL to 10 mg/mL were tested and a concentration of 4.5 mg/mL HA in PBS showed comparable viscosity to the human vitreous (at 1 Hz). This concentration was taken on for further evaluation.

For all the vitreous test samples except HA, storage and loss moduli decreased as the oscillatory stress increased Fig. 4. After the LVR, yield of the gel is observed at ~0.1 Pa for vitreous samples, manifesting as a reduction in G′ and G″ due to disruption of the gel structure. There is no significant difference in storage and loss moduli and complex viscosity of bovine, porcine and HA compared with human VH ($P > 0.05$) at low stress. At stresses under 1 Pa, G′ is greater than G″ for all samples except HA, indicating that an elastic-like behaviour dominates. Ovine VH showed a significantly higher G′ (4.2 ± 0.62 Pa) in comparison with human, bovine, porcine, and HA which had G′ measurements of 1.4 ± 0.95 Pa, 1.7 ± 0.31 Pa, 1.4 ± 0.14 Pa, and 0.7 ± 0.12 Pa respectively. For all samples except HA, as the shear stress exceeded 1 Pa, G″ values surpassed G′, indicating that the shear stresses were large enough to overcome the intramolecular forces within the structure, and the sample started to express a viscous-fluid-like behaviour and flow. In the case of HA, G″ was higher than G′ throughout the experiment and sample started to show thinning at oscillatory stress above 10 Pa. This demonstrates that whilst viscosity was comparable at low shear, as in a Franz cell, the elasticity of the mimic was lower than the vitreous'.

3.2. Rheological properties: frequency stress sweep (FSS)

During this test, the frequency varied from 0.1 to 10 Hz while the amplitude of the shear stress was kept constant at 1% strain which was found to be within the LVR. In Fig. 5, the storage [G′] and loss [G″] moduli and complex viscosity [η*] were plotted against the frequency, with data at low frequencies describing the behaviour of the vitreous samples at frequencies near rest.

As shown in Table 2, at a low frequency of 0.1 Hz, ovine vitreous had a significantly higher G′ (6.7 ± 0.48 Pa), G″ (3.7 ± 0.45 Pa), and complex viscosity (12.3 ± 0.94 Pa.s) in comparison with other samples. In addition, bovine, ovine and porcine VH had a higher complex viscosity at 0.1 Hz in comparison with complex viscosity measured with oscillatory stress test at 1 Hz. Unfortunately, due to the scarcity of the tissue, human vitreous could not be studied.

In general, ovine VH exhibited a significantly higher complex viscosity value of 12.3 ± 0.94 Pa.s for FSS test amongst all samples ($p \leq 0.01$***). In addition, there was no significant difference in

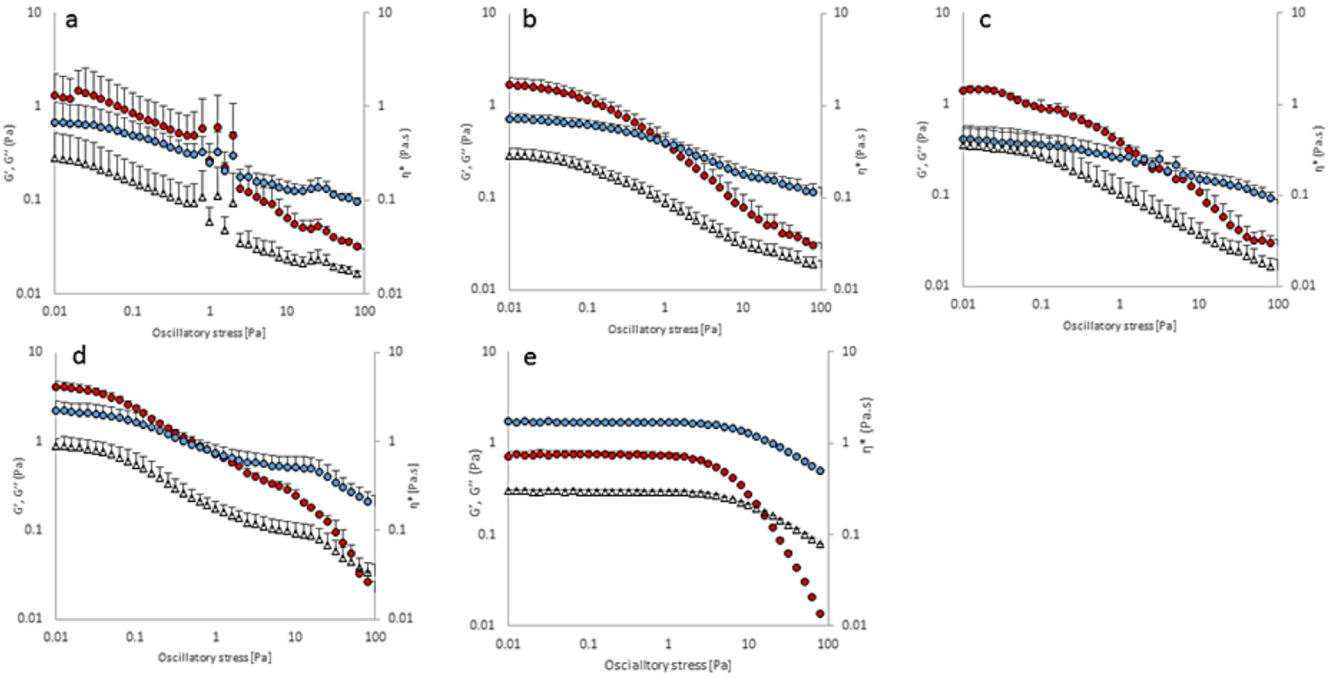

Fig 4. complex viscosity [η*] (open triangle), storage (G') (red), and loss (G") (blue) moduli vs. oscillatory stress for a) human, b) bovine, c) porcine, and d) ovine vitreous humours, and e) hyaluronic acid, at 1 Hz. Data are presented as mean + SD, n = 3. Error in Y is bidirectional, but shown only in a positive direction for clarity.

rheological characteristics of bovine, porcine, and HA when compared to human VH at the points taken. All test samples showed a higher viscosity at a lower frequency of 0.1 Hz, and frequency-dependent G′ and G″, indicating that the gels are physically entangled.

3.3. In vitro diffusion studies

A bespoke Franz cell construct was constructed to perform *in vitro* diffusion studies. Values for steady state flux, lag time and diffusion coefficients were derived from the relationship between cumulative fluorescein permeated per unit area vs. time, as shown in Fig. 6. A Franz-cell model was investigated with PBS as the control test sample which showed the shortest lag time (1.62 ± 0.03 h), significantly higher steady-state flux (55.84 ± 0.95 μg/cm^2/h) and significantly higher diffusion coefficient (231.59 ± 4.52 × 10^{-3} cm^2/h) in comparison with the rest of the samples ($p \leq 0.001$***). This demonstrates that the vitreous diffusion is rate-limiting in the diffusion experiments. However, human vitreous humour had a significantly higher steady-state flux and diffusion coefficient ($p \leq 0.001$***) in comparison with bovine, porcine, and ovine samples. Although steady-state flux was significantly higher for human than HA ($p \leq 0.001$***), there was no significant difference in their diffusion coefficient ($P > 0.05$) (Fig. 7).

3.4. Cryo-scanning electron microscope

Native human and mammalian vitreous humour, as well as HA, were assessed using cryo-SEM. It is expected the vitreous samples contain a dense network of protein fibrils (primarily collagen II) and polysaccharide chains that are primarily hyaluronan. SEM images are shown in Fig. 8. All vitreous samples had a highly porous microstructure, with average pore diameters of 74.42 ± 4.45 nm, 66.49 ± 8.91 nm, 57.14 ± 9.41 nm, 95.55 ± 9.67 nm, and 97.38 ± 32.92 nm for bovine, porcine, ovine, human, and HA, respectively, measured at ×5000 magnification using ImageJ. There is also evidence of directional striation. Although the composition of extracellular matrix elements of the vitreous gel is similar in all species, the concentration of the components such as HA and collagen varies in different species. HA showed a similar dense network of hyaluronan chains as seen in human vitreous sample Fig. 8. However, due to the fragile vitreous meshwork, samples may be affected by structural alteration and artefacts during SEM sample preparation.

4. Discussion

The vitreous humour is a viscoelastic hydrogel comprised of two main biopolymers; collagen and hyaluronan (Sharif-Kashani et al., 2011). Collagen forms fibrils, which are interspersed with hyaluronan, which maintains the structure of the gel (Swann and Sotman, 1980). In order to design an effective intravitreal drug delivery system one must be able to predict the disposition of drug in the vitreous humour (Su et al., 2015). The majority of studies of drug diffusion in the vitreal body use *ex* vivo bovine vitreous, but the similarity of this tissue to human has not been established. Thus there is a need to understand how mammalian vitreous behaves compared to human. Additionally, due to the difficulty in sourcing *ex vivo* vitreous, there is also a need to establish mimics for the vitreous which do not require collection, extraction, and storage; this could also be achieved without the need for animal tissue. There is also a need for mimics of the human vitreous for replacement of human vitreous during surgery. The most commonly used vitreous substitutes are expansile gases, silicone oil and perfluoro carbon liquids, which not mimic drug disposition in the vitreous (Donati et al., 2014). Additionally, these materials may dissolve or emulsify over time. Therefore, the search for an ideal substitute for vitreous humour is still an ongoing challenge.

In this study, a bespoke Franz-cell model was developed to evaluate diffusion through a series of vitreous humours from different species; human, bovine, porcine, and ovine, and a vitreous mimic, HA. In addition, the rheological properties of these test samples were evaluated. To characterise the visco-elastic behaviour of the VH, most studies focus on the measurement of the VH storage moduli, known as G′, and loss moduli, known as G″ (Filas et al., 2014; Silva et al., 2017). The storage moduli represents the elastic or recoverable component, while the loss moduli, illustrates the viscous component related to the dissipated energy (Silva et al., 2017).

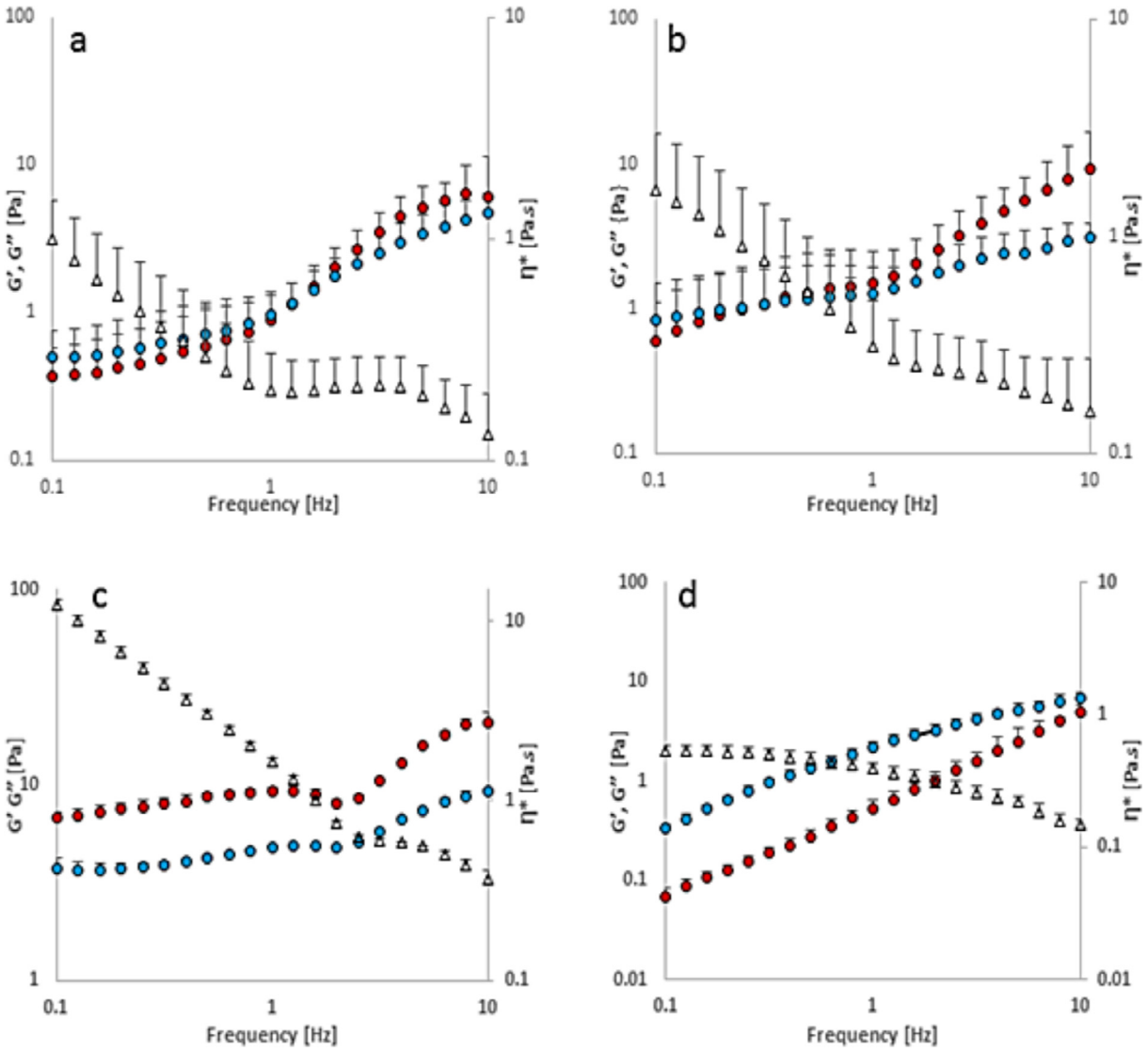

Fig 5. complex viscosity [η*] (open triangle), storage (G′) (red), and loss (G″) (blue) modulus vs. frequency [Hz] for a) bovine, b) porcine, and C) ovine vitreous humours and d) hyaluronic acid, at frequency range of 0.1–10 Hz. Data are presented as mean + SD, n = 3. Error in Y is bidirectional, but shown only in a positive direction for clarity. (For interpretation of the references to colour in this figure legend, the reader is referred to the web version of this article.)

Oscillatory stress sweeps were performed to observe the behaviour of the vitreous samples as the amplitude of the applied shear stress was increased. All vitreous samples demonstrated a yield and thinning by 1 Pa, indicating that shear force overcame the intermolecular forces within the samples' structure, G″ values surpassed G′, indicating an end to gel-like elastic behaviour and the onset of fluid-like flow. As seen in Table 1, the approximate rank order of vitreous collagen concentrations are porcine < bovine < ovine, which is mirrored in their values of G' as shear stress approaches zero, suggesting that the gel properties are primarily determined by the collagen fibrils (Silva et al., 2017). This rank order is also reflected in their values of compressive hardness. A study by Sakuma et al. (2004), supported this idea, as digesting vitreous humour with collagenase resulted in reduction of vitreous gel elasticity, indicating the elastic properties of vitreous to be mostly associated with collagen fibrils. In addition, another study by Filas et al. (2014), showed higher storage moduli for bovine VH than porcine samples, by digesting VH samples with collagenase and hyaluronidase to see a more liquid and solid like property, respectively. The measured rheological

Table 2
complex viscosity [η*], storage [G′] and loss [G″] modulus measurements for oscillatory stress sweep test taken at Linear Viscoelastic Region (LVR) for various vitreous humour samples at 1 Hz and frequency stress sweep test at 0.1 Hz. Hardness (N) of the samples are tested using texture profile analyser. Data are presented as mean ± SD, n = 3.

Sample	G′ [Pa] (1 Hz)	G′ [Pa] (0.1 Hz)	G″ [Pa] (1 Hz)	G″ [Pa] (0.1 Hz)	[η*] (1 Hz)	[η*] (0.1 Hz)	Hardness (N)
Human	1.4 ± 0.95	–	0.7 ± 0.37	–	0.3 ± 0.25	–	–
Bovine	1.7 ± 0.31	0.4 ± 0.19	0.7 ± 0.12	0.5 ± 0.25	0.3 ± 0.05	0.9 ± 0.51	10.9 ± 0.36
Porcine	1.4 ± 0.14	0.6 ± 0.49	0.4 ± 0.14	0.8 ± 0.66	0.3 ± 0.07	1.6 ± 1.32	6.4 ± 0.84
Ovine	4.2 ± 0.62	6.7 ± 0.48	2.3 ± 0.56	3.7 ± 0.45	0.9 ± 0.24	12.3 ± 0.94	21.2 ± 0.71
HA	0.7 ± 0.12	0.05 ± 0.02	1.7 ± 0.04	0.3 ± 0.03	0.3 ± 0.01	0.5 ± 0.05	12.1 ± 3.41

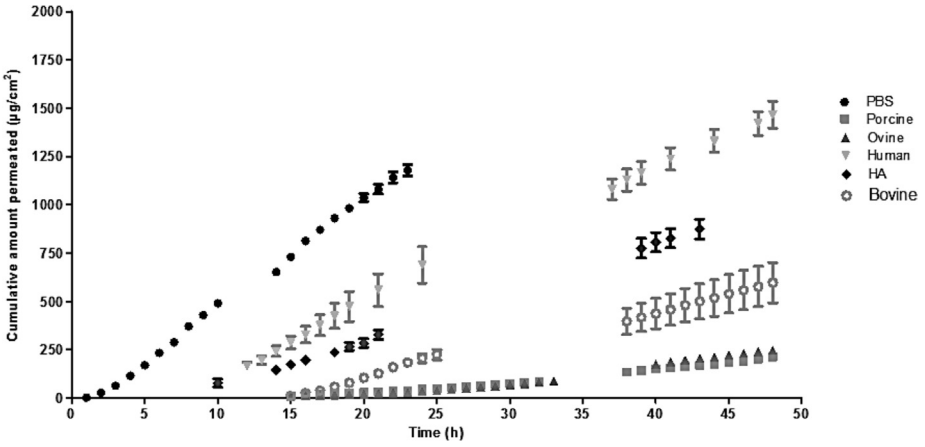

Fig 6. Cumulative amount of fluorescent dye permeated through a semi-permeable membrane known as Visking Dialysis Tubing membrane with different samples in the middle compartment of Franz cell including PBS (control), bovine, porcine, and ovine vitreous humours and HA (4.5 mg/ml in PBS). Data are presented as mean ± SD, n = 3. The lag time (h) can be calculated by extrapolation of the steady state region to y = 0. Therefore, for each sample, the lag time is calculated via the line of best fit from the steady state region where the cumulative fluorescein permeated per unit area is zero (y = 0).

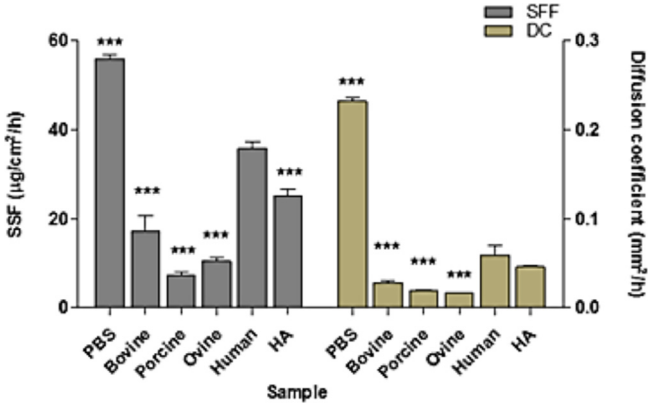

Fig 7. Steady-state flux (SSF) and diffusion coefficient (DC) measurements related to PBS, bovine, porcine, ovine, and human vitreous humours, and hyaluronic acid (4.5 mg/mL in PBS) are compared. Data are analysed using One-way ANOVA with Bonferroni post-hoc test and presented as mean + SD, n = 3. Error in Y is bidirectional, but shown only in a positive direction for clarity. Any significant difference in results is shown as $p \leq 0.05$*, $p \leq 0.01$**, $p \leq 0.001$*** and is relative to human vitreous humour.

properties of human vitreous were most comparable to the bovine and porcine vitreous, with ovine demonstrating greater G′, G″, and viscosity. From the data collected, a 4.5 mg/mL HA sample of matched viscosity to the human vitreous was prepared, to be explored as a first-generation vitreous mimic.

After the fluid's linear viscoelastic region has been defined by a strain sweep, its structure can be further characterized using a frequency sweep at a strain below the critical strain, within the LVR. Below the critical strain, the more frequency dependent the elastic modulus is, the more fluid-like is the material (Franck, 2004). The dependence of all vitreous samples' viscoelasticity on frequency is indicative of a structure maintained by entanglements, rather than chemical cross-links. At both low and high frequencies, ovine vitreous humour showed the highest values for G′, G″, and complex viscosity [η*] amongst all samples. In general, increasing the frequency had a thinning effect on the samples.

The vitreous humour fills the vitreous cavity of the eye and modulates the diffusion of molecules, such as drugs, oxygen and growth factors. The Stokes–Einstein equation suggests that the rate of transport of any substance by diffusion is inversely related to the viscosity of the medium (Gisladottir et al., 2009; Stefansson and Loftsson, 2006). Ovine VH with the highest G′, exhibited the highest complex viscosity value of 0.9 ± 0.24 Pa.s and 12.3 ± 0.94 Pa.s for OSS and FSS tests amongst all samples. In addition, the viscosity of bovine and porcine vitreous samples, 0.3 ± 0.05 Pa.s and 0.2 ± 0.07 Pa.s values respectively, were similar to the viscosity of human vitreous with a value of 0.3 ± 0.25 Pa.s. All the vitreous samples showed a higher viscosity at a lower frequency. Although for porcine and bovine samples, G' was lower at 0.1 Hz in comparison with OSS results at 1 Hz, the opposite is seen for ovine samples which showed higher G′, G″, and complex viscosity at a lower frequency, 0.1 Hz.

The diffusion of fluorescein through vitreous samples was studied to

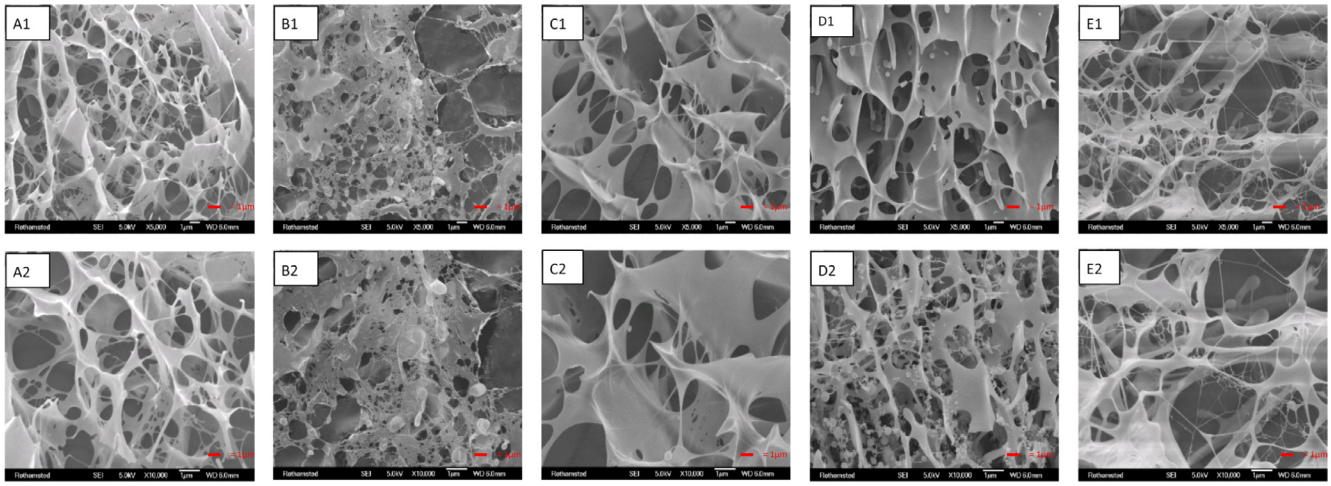

Fig 8. Cryo-scanning electron micrographs (cryo-SEM) of A) human, B) bovine, C) porcine, D) ovine vitreous humours, and E) hyaluronic acid at low magnification (group 1 × 5000) and high magnification (group 2 × 10000). Scale bar represents 1 µm.

determine the similarity of animal vitreous to human, in this respect. A 4.5 mg/mL HA solution with matched viscosity (at 1 Hz) to human vitreous was also evaluated as a potential surrogate. PBS was used as a control to confirm that diffusion through the vitreous was rate-limiting.

The results indicated a significantly higher steady-state flux and diffusion coefficient through PBS ($p \leq 0.001$) in comparison with all vitreous samples and HA, confirming that the diffusion cell set-up was not limiting diffusion. Although human, bovine and porcine vitreous humours showed similar rheological properties, steady state flux through bovine vitreous was significantly higher than porcine ($p \leq 0.01$), and flux through the human vitreous was significantly ($p < 0.001$) greater than both. In contrast, ovine with highest G′, G″, and complex viscosity showed a significantly lower flux in comparison with bovine ($p \leq 0.05$) and human ($p < 0.01$), but not porcine. However, human vitreous humour with a complex viscosity similar to that of bovine (0.3 Pa.s) had a significantly higher rate of diffusion and flux ($p < 0.001$). Therefore, it can be suggested that solute's diffusion is not only affected by viscosity of the medium, but also a contribution of other factors including solute concentration, interactions between drug and diffusion medium, and the diffusion network mesh size (Santoro et al., 2011), as well as gel related factors including tortuosity of the sample (Tong and Anderson, 1996). Furthermore, age-related changes in vitreal structure including vitreous liquefaction, fibre aggregation, and reorganisation of the hyaluronic acid and collagen network can also affect solute's diffusion (Spitzer and Januschowski, 2015). For instance, aging results in the aggregation of vitreous collagen fibrils due to a loss of collagen components which are necessary for maintaining a gelatinous non-liquified state in vitreous (Meral and Bilgili, 2011). In addition, diffusion of solutes in the vitreous humour has been shown to be affected by the particle's surface charge; a positively charged particle will be trapped and localised into the three dimensional collagen fibril networks in comparison with positively charged solutes (Koo et al., 2012).

When diffusion coefficients were calculated, the rank order of diffusivity was human > bovine > porcine > ovine. The best surrogate for human vitreous in these experiments was 4.5 mg/mL HA, which gave significantly lower values of steady state flux, but values of fluorescein diffusion coefficient which were not statistically significant from those measured in the human vitreous.

5. Conclusions

Animal models of the vitreous are often used as surrogates for human samples when testing the diffusion of drugs through the vitreal body, but there exists little evidence that they are reliable mimics. The rheological properties of human, porcine, and bovine vitreous are comparable, but ovine vitreous has greater elasticity and viscosity. The diffusion of fluorescein through the different vitreous samples revealed great differences in values of steady-state flux and diffusion coefficient. The rate of fluorescein diffusion through the human vitreous was greater than in the other samples, indicating that results of previous diffusion studies in non-human models may not be translatable to humans. Where surrogates for the human vitreous are required for these studies, a first-generation vitreous mimic, composed of 4.5 mg/mL hyaluronic acid has been evaluated, which was a closer mimic of the human vitreous than the mammalian samples investigated, under these conditions.

Acknowledgements

Human tissue for this project was provided by Moorfields Biobank and supported by National Institute of Health Research (NIHR), United Kingdom, funding. The authors would like to thank Dr Rebecca Lauder, Rothamsted Institute, for her technical assistance and advice during the SEM.

References

Balazs, E.A., Laurent, T.C., Laurent, U.B., 1959. Studies on the structure of the vitreous body VI. Biochemical changes during development. J. Biol. Chem. 234 (2), 422–430.
Bishop, P.N., 2000. Structural macromolecules and supramolecular organisation of the vitreous gel. Prog. Retinal Eye Res. 19 (3), 323–344.
Bishop, P.N., Holmes, D.F., Kadler, K.E., McLeod, D., Bos, K.J., 2004. Age-related changes on the surface of vitreous collagen fibrils. Invest. Ophthalmol. Visual Sci. 45 (4), 1041–1046.
Denlinger, J.L., Eisner, G., Balazs, E.A., 1980. Age-related changes in the vitreus and lens of rhesus monkeys (Macaca mulatta). Exp. Eye Res. 31 (1), 67–79.
Donati, S., Caprani, S.M., Airaghi, G., Vinciguerra, R., Bartalena, L., Testa, F., et al., 2014. Vitreous substitutes: the present and the future. BioMed Res. Int.
Duvvuri, S., Majumdar, S., Mitra, A.K., 2003. Drug delivery to the retina: challenges and opportunities. Expert Opin. Biol. Ther. 3 (1), 45–56.
Eriksen, A.Z., Brewer, J., Andresen, T.L., Urquhart, A.J., 2017. The diffusion dynamics of PEGylated liposomes in the intact vitreous of the ex vivo porcine eye: a fluorescence correlation spectroscopy and biodistribution study. Int. J. Pharm. 522 (1–2), 90–97.
Filas, B.A., Zhang, Q., Okamoto, R.J., Shui, Y.-B., Beebe, D.C., 2014. Enzymatic degradation identifies components responsible for the structural properties of the vitreous bodystiffness and adhesivity of the vitreous. Invest. Ophthalmol. Visual Sci. 55 (1), 55–63.
Franck, A., 2004. Understanding rheology of structured fluids. Book of TA instruments. pp. 1–17.
Gisladottir, S., Loftsson, T., Stefansson, E., 2009. Diffusion characteristics of vitreous humour and saline solution follow the Stokes Einstein equation. Graefe's Arch. Clin. Exp. Ophthalmol. 247 (12), 1677–1684.
Green, W., Sebag, J., 2006. Vitreoretinal interface. Retina 3, 1921–1989.
Käsdorf, B.T., Arends, F., Lieleg, O., 2015. Diffusion regulation in the vitreous humor. Biophys. J. 109 (10), 2171–2181.
Kodama, M., Matsuura, T., Hara, Y., 2013. Structure of vitreous body and its relationship with. Liquefaction.
Kogan, G., Šoltés, L., Stern, R., Gemeiner, P., 2007. Hyaluronic acid: a natural biopolymer with a broad range of biomedical and industrial applications. Biotechnol. Lett. 29 (1), 17–25.
Koo, H., Moon, H., Han, H., Na, J.H., Huh, M.S., Park, J.H., et al., 2012. The movement of self-assembled amphiphilic polymeric nanoparticles in the vitreous and retina after intravitreal injection. Biomaterials 33 (12), 3485–3493.
Landers 3rd, M.B., Watson, J.S., Ulrich, J.N., Quiroz-Mercado, H., 2012. Determination of retinal and vitreous temperature in vitrectomy. Retina 32 (1), 172–176.
Le Goff, M., Bishop, P., 2008. Adult vitreous structure and postnatal changes. Eye 22 (10), 1214.
Loch, C., Nagel, S., Guthoff, R., Seidlitz, A., Weitschies, W., 2012. The Vitreous Model – a new in vitro test method simulating the vitreous body. Biomed. Eng./Biomed. Tech. 57 (SI-1 Track-O), 281–284.
Meral, I., Bilgili, Y., 2011. Diffusion changes in the vitreous humor of the eye during aging. Am. J. Neuroradiol. 32 (8), 1563–1566.
Nickerson, C.S., Park, J., Kornfield, J.A., Karageozian, H., 2008. Rheological properties of the vitreous and the role of hyaluronic acid. J. Biomech. 41 (9), 1840–1846.
Noulas, A.V., Skandalis, S.S., Feretis, E., Theocharis, D.A., Karamanos, N.K., 2004. Variations in content and structure of glycosaminoglycans of the vitreous gel from different mammalian species. Biomed. Chromatogr. 18 (7), 457–461.
Ohtori, A., Tojo, K., 1994. In vivo/in vitro correlation of intravitreal delivery of drugs with the help of computer simulation. Biol. Pharm. Bull. 17 (2), 283–290.
Pirie, A., Schmidt, G., Waters, J., 1948. Ox vitreous humour. 1.—The residual protein. Br. J. Ophthalmol. 32 (6), 321.
Reardon, A., Heinegård, D., Mcleod, D., Sheehan, J.K., Bishop, P.N., 1998. The large chondroitin sulphate proteoglycan versican in mammalian vitreous. Matrix Biol. 17 (5), 325–333.
Rosa, M.F., Scano, P., Noto, A., Nioi, M., Sanna, R., Paribello, F., et al., 2015... Monitoring the modifications of the vitreous humor metabolite profile after death: an animal model. BioMed Res. Int.
Sakuma, T., Won, Y.Y., Sueda, J., Usumoto, N., Weitz, D., Hirose, T., 2004. Rheology of vitreous: effects of enzymes. Invest. Ophthalmol. Visual Sci. 45 (13), 1948.
Santoro, M., Marchetti, P., Rossi, F., Perale, G., Castiglione, F., Mele, A., et al., 2011. Smart approach to evaluate drug diffusivity in injectable agar− carbomer hydrogels for drug delivery. J. Phys. Chem. B 115 (11), 2503–2510.
Scott, J.E., 1992. The chemical morphology of the vitreous. Eye 6 (6), 553.
Sebag, J., Balazs, E., 1989. Morphology and ultrastructure of human vitreous fibers. Invest. Ophthalmol. Visual Sci. 30 (8), 1867–1871.
Shafaie, S., Hutter, V., Cook, M.T., Brown, M.B., Chau, D.Y., 2016. In Vitro cell models for ophthalmic drug development applications. BioRes. Open Access. 5 (1), 94–108.
Sharif-Kashani, P., Hubschman, J.-P., Sassoon, D., Kavehpour, H.P., 2011. Rheology of the vitreous gel: effects of macromolecule organization on the viscoelastic properties. J. Biomech. 44 (3), 419–423.
Silva, A.F., Alves, M.A., Oliveira, M.S., 2017. Rheological behaviour of vitreous humour. Rheol. Acta 56 (4), 377–386.
Spitzer, M.S., Januschowski, K., 2015. Aging and age-related changes of the vitreous body. Der Ophthalmol.: Z. Deutschen Ophthalmol. Gesellschaft 112 (7), 552 4–8.
Stefansson, E., Loftsson, T., 2006. The Stokes−Einstein equation and the physiological effects of vitreous surgery. Acta Ophthalmol. 84 (6), 718–719.
Su, X., Tan, M.J., Li, Z., Wong, M., Rajamani, L., Lingam, G., et al., 2015. Recent progress in using biomaterials as vitreous substitutes. Biomacromolecules 16 (10), 3093–3102.
Swann, D.A., Sotman, S.S., 1980. The chemical composition of bovine vitreous-humour collagen fibres. Biochem. J 185 (3), 545–554.

Tan, L.E., Orilla, W., Hughes, P.M., Tsai, S., Burke, J.A., Wilson, C.G., 2011. Effects of vitreous liquefaction on the intravitreal distribution of sodium fluorescein, fluorescein dextran, and fluorescent microparticles. Invest. Ophthalmol. Visual Sci. 52 (2), 1111–1118.

Tong, J., Anderson, J.L., 1996. Partitioning and diffusion of proteins and linear polymers in polyacrylamide gels. Biophys. J. 70 (3), 1505–1513.

Vedadghavami, R., 2015. Rheology of Vitreous Gel. University of California, Los Angeles.

Xu, Q., Boylan, N.J., Suk, J.S., Wang, Y.-Y., Nance, E.A., Yang, J.-C., et al., 2013. Nanoparticle diffusion in, and microrheology of, the bovine vitreous ex vivo. J. Control. Release 167 (1), 76–84.

Xu, J., Heys, J.J., Barocas, V.H., Randolph, T.W., 2000. Permeability and diffusion in vitreous humor: implications for drug delivery. Pharm. Res. 17 (6), 664–669.